

PLASTIC PROPERTIES AND MICROSTRUCTURE EVOLUTION OF 20CrMoA STEEL DURING WARM DEFORMATION

Received – Priljeno: 2021-11-09

Accepted – Prihvaćeno: 2022-03-10

Original Scientific Paper – Izvorni znanstveni rad

The plastic properties and microstructure evolution of 20CrMoA steel was analyzed at 600–750 °C and strain rate of 0,01–10 s⁻¹. The result reveals that the deformation behavior is hardening followed by softening at low strain rates (0,01 s⁻¹ and 0,1 s⁻¹), but hardening is dominant in the whole deformation process at high strain rates (1 s⁻¹ and 10 s⁻¹) and low temperature (600 °C and 650 °C). The strain rate sensitivity exponent increases with the increasing deformation temperature except for 650 °C and high strain rate. The spheroidization mechanism of cementite is the mechanical fracture and the dissolution of cementite particles. At 700 °C, spheroidized particles are finer and their distribution is more uniform than that at 750 °C.

Keywords: 20CrMoA steel, warm deformation, plastic properties, strain-stress curves, microstructure evolution

INTRODUCTION

Warm forming has been studied on various carbon steels. The strength of carbon steel can be greatly improved during warm forming but at the cost of ductility and toughness [1]. In studying the warm forming, the deformation often occurred in the dual-phase region. Recrystallization and recovery occurred simultaneously and interacted with each other, and their speed and share in microstructural variation depended on the initial microstructure and process parameters [2]. These will have a great impact on the flow behavior of the material. Therefore, it is necessary to combine the flow stress behavior and microstructure evolution to analyze the plastic properties of the materials, and finally determine the appropriate parameters for warm forming process.

In this paper, low-carbon and low-alloy steel 20CrMoA with the initial microstructure of ferrite and pearlite was selected to investigate its warm deformation behavior and plastic properties by compression tests.

EXPERIMENTAL PROCEDURES

The chemical composition (in wt.%) of 20CrMoA steel was 0,2 C - 0,24 Si - 0,52 Mn - 0,92 Cr - 0,16 Mo and Fe balance. The specimen size is $\Phi 8 \times 12$ mm and the simulation experiments were performed on a Gleeble - 3500 thermal simulator. The deformation temperatures were 600 °C, 650 °C, 700 °C and 750 °C. The

strain rates were of 0,01 s⁻¹, 0,1 s⁻¹, 1 s⁻¹ and 10 s⁻¹. Each specimen was heated to the specified deformation temperature at rate of 10 °C / s and held for 3 min under

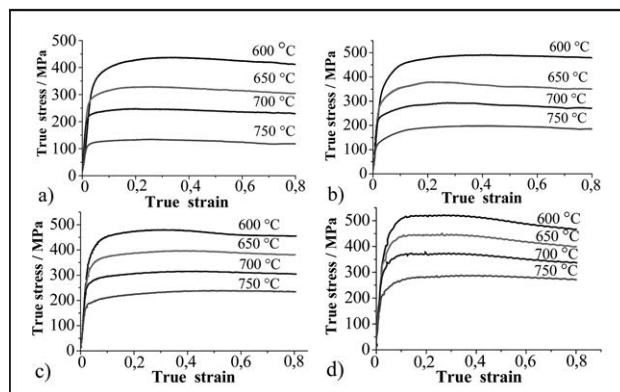


Figure 1 True stress–strain curves under different conditions. (a) 0,01 s⁻¹; (b) 0,1 s⁻¹; (c) 0,1 s⁻¹; (d) 0,01 s⁻¹

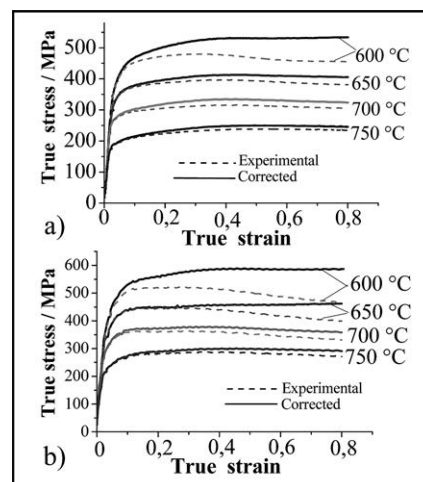


Figure 2 Corrected true stress curves. (a) 1 s⁻¹; (b) 10 s⁻¹

Sh. Xu, X. D. Shu : shuxuedao@nbu.edu.cn, Ningbo University, School of Mechanical Engineering and Mechanics, Ningbo, China

Sh. Xu, ZH. L. Shen, L. J. Zhu, Department of Mechanical Engineering, Zhejiang Business and Technology Institute, Ningbo, China.

J. Zhao, Ningbo Sub-Academy of the national weapons science research academy, Ningbo, China.

isothermal conditions for reaching heat balance. The height was reduced by 70 %.

TRUE STRESS-STRAIN CURVES

Figure 1 shows the true stress-strain curves. At the initial stage of deformation, the stress increases rapidly to a peak then is stable. At low temperature (600 °C and 650 °C) and high strain rate (1 s⁻¹ and 10 s⁻¹), the stress decreases with the increasing strain. The main reason is that the specimen temperature rose due to the deformation heat at high strain rate, resulting in material softening. During the deformation, most of the energy is converted into heat energy. At a high strain rate, most of the deformation heat cannot be dissipated timely, but be stored as heat energy, leading to the temperature rise of specimen and reduction of stress [3].

The effect of temperature rise on flow stress of 20CrMoA steel is expressed as [4]:

$$\Delta\sigma = \frac{652,61}{14,67 \times 0,00246} \left(\frac{1}{T} - \frac{1}{T + \Delta T} \right) \quad (1)$$

Where, $\Delta\sigma$ is the effect of temperature rise on stress; T is temperature (K); ΔT is temperature rise. Substituting Equation (1) with the temperature rise, the corrected true stress curves at high strain rate can be obtained, as shown in Figure 2.

TEMPERATURE SENSITIVITY

The temperature sensitivity can be determined by the following expression[5]:

$$q = \left(\frac{\partial \log \sigma}{\partial \log T} \right)_{\varepsilon, \dot{\varepsilon}} \quad (2)$$

The result shows that the value of temperature sensitivity q is negative. The absolute value of q reflects the degree to the variation of stress with the temperature. As shown in Figure 3, the absolute value of q at strain of 0,3 increases with the increasing temperature due to the great softening effect at high temperature, and decreases with the increasing strain rate. The main reason is that the effect of deformation temperature on energy accumulation and dynamic softening reduces due to short time.

At strain of 0,3, the corresponding stress values at 0,01 s⁻¹, 0,1 s⁻¹, 1 s⁻¹ and 10 s⁻¹ decrease by 67,94 %, 59,71 %, 53,69 % and 48,97 % respectively when the temperature increases from 600 °C to 750 °C. The temperature sensitivity is very distinct at 0,01 s⁻¹. The temperature sensitivity at 650 °C is almost equal to that at 600 °C, but lower than that at 700 °C and 750 °C. In addition, the variation of absolute value of q at 0,01 s⁻¹ is also much larger than that at other conditions. The longer deformation time enhances the thermal softening effect.

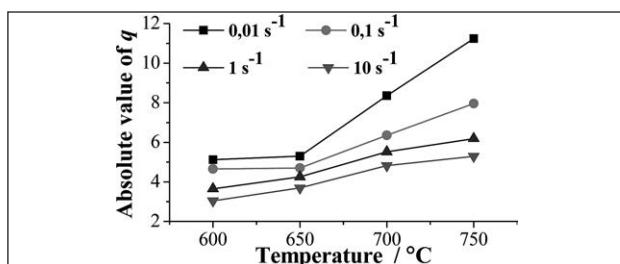


Figure 3 The relationship between absolute value of q and deformation temperature (strain=0,3).

59,71 %, 53,69 % and 48,97 % respectively when the temperature increases from 600 °C to 750 °C. The temperature sensitivity is very distinct at 0,01 s⁻¹. The temperature sensitivity at 650 °C is almost equal to that at 600 °C, but lower than that at 700 °C and 750 °C. In addition, the variation of absolute value of q at 0,01 s⁻¹ is also much larger than that at other conditions. The longer deformation time enhances the thermal softening effect.

STRAIN HARDENING EXPONENT

Strain hardening exponent can be calculated as [5]:

$$n_d = \left(\frac{\partial \log \sigma}{\partial \log \varepsilon} \right)_{\dot{\varepsilon}, T} \quad (3)$$

Where, σ is true stress (MPa); T is deformation temperature (K); ε is true strain and $\dot{\varepsilon}$ is strain rate.

As shown in Figure 4, the n_d value is always negative when the strain is more than 0,5 except for low temperature and high strain rates. The mechanism is the competition between dislocation accumulation and dislocation annihilation. In the early stage of deformation, dislocation accumulation is higher than the dislocation annihilation, resulting in increase in dislocation density and work hardening. Therefore, the dominant mecha-

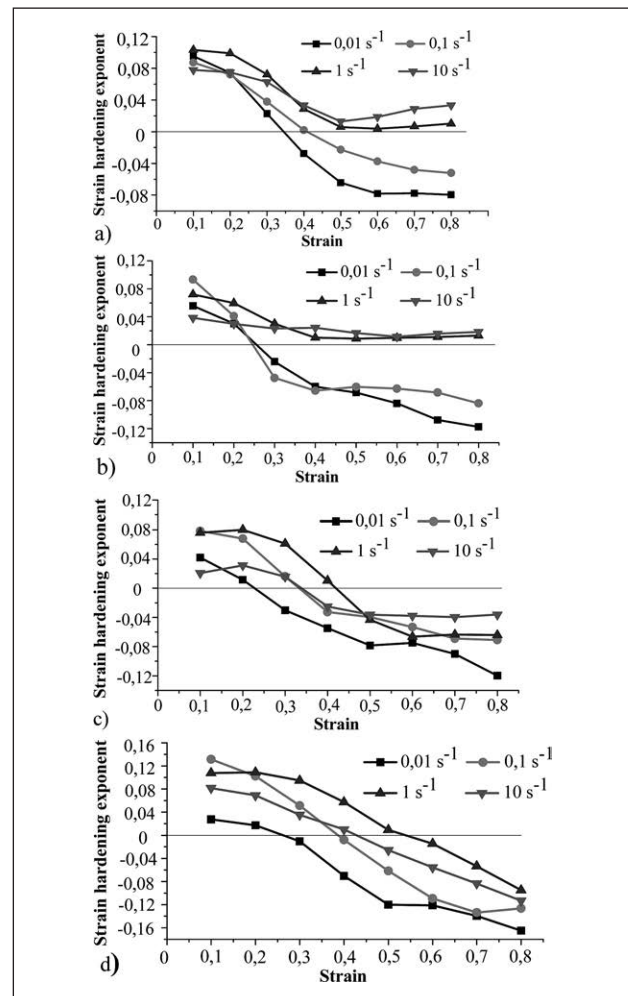


Figure 4 The relationship between strain and strain hardening exponent. (a) 600 °C; (b) 650 °C; (c) 700 °C; (d) 750 °C

nism is hardening in the initial stage, but softening in the late stage. However, weak thermal effect at low temperature and shorter deformation time caused by low strain rate lead to the dominant effect of hardening.

STRAIN RATE SENSITIVITY

Similarly, the strain rate sensitivity exponent can be expressed as:

$$m = \left(\frac{\partial \log \sigma}{\partial \log \dot{\epsilon}} \right)_{\epsilon, T} \quad (4)$$

The results make clear that strain rate sensitivity exponent m is positive as shown in Figure 5. In Figure 5(a) and 5(b), the strain rate sensitivity increases with the increasing strain and the increase rate is approximate. At high strain rates, the m value decreases firstly and then stays in a relatively stable range, in addition, at a fixed strain rate, the m value increases with the increasing temperature except for the values at 650 °C and high strain rates, as shown in Figure 5(c) and Figure 5(d).

The variation of m value at 650 °C is more than 700 °C, especially the m values are larger when the strain is

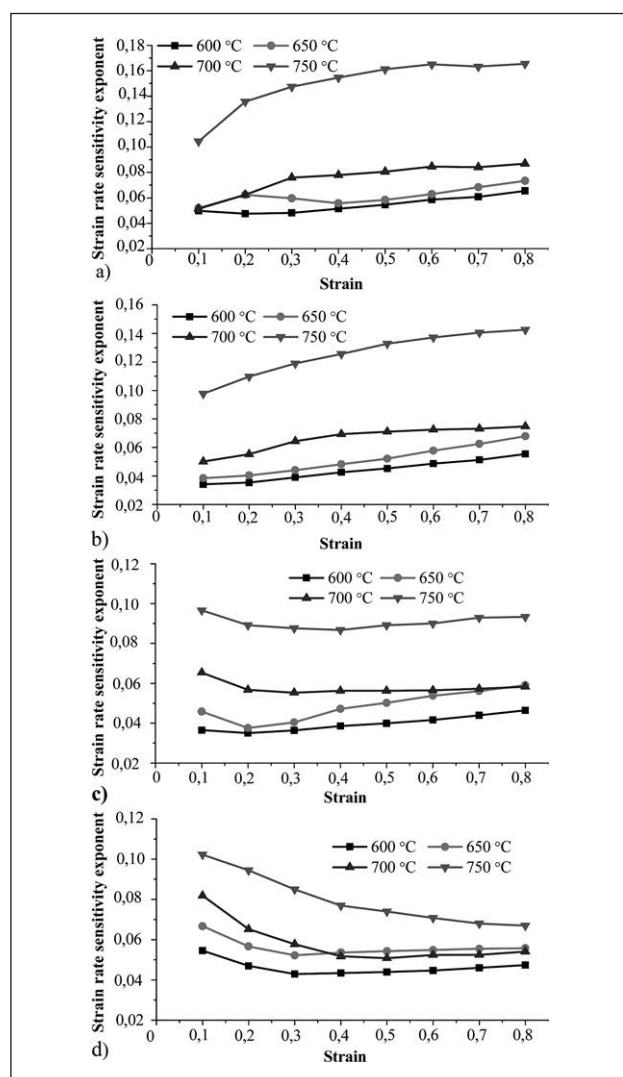


Figure 5. Strain rate sensitivity exponent. (a) 0,01 s⁻¹; (b) 0,01 s⁻¹; (c) 0,01 s⁻¹; (d) 0,1 s⁻¹

more than 0,4 at 10 s⁻¹. The strain hardening curves and the stress curves can reveal the cause of this phenomenon. In the late stage of deformation at high strain rate, the dominant role is hardening at 650 °C, but is softening at 700 °C as shown in Figure 4(b) and 4(c), furthermore, according to the stress curves, the increase of the stress caused by hardening is larger than the decrease caused by softening, which means that at high strain rates the critical deformation temperature range from hardening to softening is between 650 °C and 700 °C, where the strain rate sensitivity decrease with the increasing temperature in the late stage of deformation. Therefore, 700 °C is more suitable for heavy deformation with large strain rate during warm deformation.

MICROSTRUCTURE EVOLUTION

Figure 6 illustrates optical micrographs under different deformation conditions. With the increasing temperature, the ferrite is deformed into long strip and the proportion of fine grain increases, which means that local recrystallization occurs. Figure 6(d) reveals that recrystallization is apparent and the grain size of ferrite decreases significantly. Compared with the microstructure at 10 s⁻¹, it is known that at 600 °C, the microstructure is still mainly coarse ferrite grain, without significant difference from that shown in Figure 6(a). In Figure 6(f), the grain size at 750 °C is obviously smaller than that at 600 °C.

The microstructure evolution shows that there is no dynamic recrystallization at 600 °C and 10 s⁻¹, but the softening characteristics of the original stress curve are the most obvious. It is also proved that plastic heat lead to the softening effect of the initial stress curves at low temperature and high strain rates.

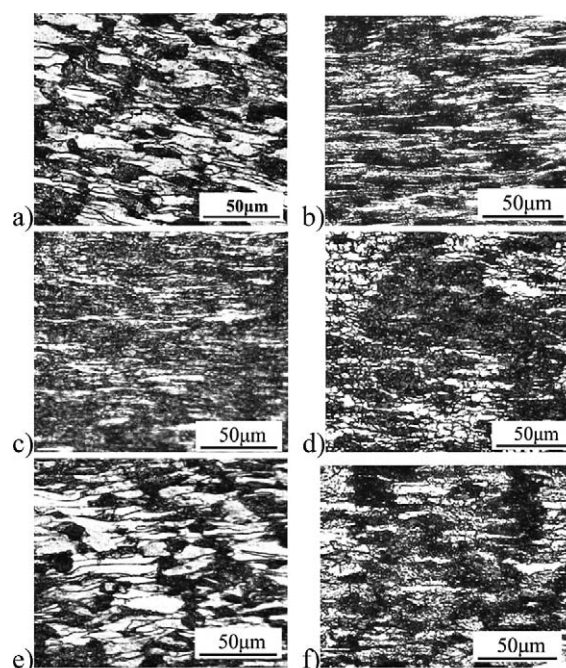


Figure 6 Optical micrographs under different deformation conditions. (a) 600 °C and 0,01 s⁻¹; (b) 650 °C and 0,01 s⁻¹; (c) 700 °C and 0,01 s⁻¹; (d) 750 °C and 0,01 s⁻¹; (e) 600 °C and 10 s⁻¹; (f) 750 °C and 10 s⁻¹

SEM micrographs in Figure 7 shows that there are visible fragments and particles resulting from fracture and spheroidization of cementite. At 600 °C, the cementite is mainly broken fragments (shown by double arrows) and a few short rods (shown by single arrow), but the distribution of short rods obviously increases at 650 °C, as shown in Figure 7(a) and Figure 7(b).

The ferrite and cementite in pearlite can be deformed coordinately at small strain, however, during heavy deformation, the coordinative deformation state will be broken due to significant difference in the mechanical properties between ferrite and cementite. Cementite will be bent, melted and spheroidized. At low temperature, the cementite is fractured under strong plastic deformation force and the fragments are in heterogeneous nucleation. At high temperature, the lamellar cementite gradually dissolves and shrinks to short rods under the driving of interface energy. Hence, more pieces of short rod cementite are produced at 650 °C than that at 600 °C at the same strain rate.

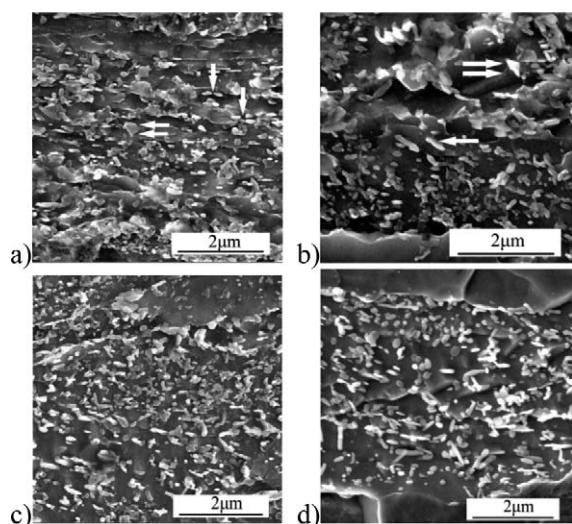


Figure 7 SEM micrographs under different conditions. (a) 600 °C and 0,01 s⁻¹; (b) 650 °C and 0,01 s⁻¹; (c) 700 °C and 10 s⁻¹; (d) 750 °C and 0,1 s⁻¹

At 700 °C and 10 s⁻¹, the spheroidized cementite particles with average diameter of 160 nm are smaller and more uniformly distributed than that with average diameter of 215 nm at 750 °C and 0.1 s⁻¹. The main mechanism is that a large number of dislocations are produced in the ferrite, providing a channel for the rapid diffusion of carbon atoms. Subsequently, the increase of deformation temperature further intensifies the diffusion, causing the concentration gradient of carbon. When the carbon gets oversaturated in the ferrite, the fine cementite particles are precipitated. 750 °C is more

favorable for diffusion of carbon atoms than 700 °C and the deformation time is longer at 0,1 s⁻¹, which is beneficial to the growth of spheroidized particles. But at high strain rate, there is not enough time for the spheroidized cementite particles to aggregate and grow. Therefore, the cementite particles at 10 s⁻¹ are obviously smaller than that at 0,01 s⁻¹.

CONCLUSIONS

At 600 °C and 650 °C, cementite in the microstructure is subject to mechanical fracture and formed into thick short rods. At 700 °C, local recrystallization occurs and small grains appear, and the cementite fragments are dissolved and spheroidized, forming into uniform and fine particles.

At 700 °C, the main mechanism is softening in the late stage of large strain rate deformation, and the strain rate sensitivity is smaller than that at 650 °C, in addition, finer and more uniformly distributed spheroidized particles can be obtained at 700 °C than at 750 °C. Hence, 700 °C is suitable for large strain rate and heavy warm deformation.

Acknowledgements

This research was funded by Research Program of Zhejiang Province (LGG20E050001), Research and Innovation Team Project of Zhejiang Business Technology Institute (KYTD202101).

REFERENCES

- [1] Hawkins D N; Shuttleworth A A. The effect of warm rolling on the structure and properties of a low-carbon steel. *Journal of Mechanical Working Technology*, 2(1979)4,333-345.
- [2] A. Niechajowicz; A. Tobota. Warm deformation of carbon steel. *Journal of Materials Processing Technology*, 106 (2000)1-3,123-130.
- [3] Wang, C.; Yu, F. et al. L. Hot deformation and processing maps of DC cast Al-15%Si alloy. *Materials Science and Engineering: A*, 577 (2013) 10, 73–80.
- [4] Xu S; Shu X; Li S; et al. Flow Stress Curve Modification and Constitutive Model of 20CrMoA Steel during Warm Deformation. *Metals*, 10(2020)1602.
- [5] Luo J; Li M Q. Strain rate sensitivity and strain hardening exponent during the isothermal compression of Ti60 alloy. *Materials Science and Engineering: A*, 538 (2012)15, 156-163.

Note: The responsible translator for the English language is Sh.Xu, Ningbo, China.